DALTON
FULL PAPER

Structural difference due to intramolecular stacking interactions in dinuclear rhodium(III) complexes $[\{Rh(\eta^5\text{-}C_5Me_5)(L)\}_2]^{n+}$ containing pyrimidine-2-thionate and related ligands

Kazuaki Yamanari,*[a] Ito Fukuda,[a] Shiori Yamamoto,[a] Yoshihiko Kushi,[a] Akira Fuyuhiro,[a] Naoko Kubota,[b] Tsuyoshi Fukuo[b] and Ryuichi Arakawa[b]

[a] *Department of Chemistry, Graduate School of Science, Osaka University, 1-16 Machikaneyama-cho, Toyonaka, Osaka 560-0043, Japan. E-mail: yamanari@ch.wani.osaka-u.ac.jp*
[b] *Department of Applied Chemistry, Kansai University, 3-3-35 Yamate-cho, Suita, Osaka 564-8680, Japan*

Received 6th January 2000, Accepted 2nd May 2000
Published on the Web 6th June 2000

Self-assembling reactions between $[Rh(\eta^5\text{-}C_5Me_5)(H_2O)_3]^{2+}$ and pyrimidine-2-thionate (pymt) or related ligands [L; mpymt = 4-methyl-pyrimidine-2-thionate(1−), dmpymt = 4,6-dimethylpyrimidine-2-thionate(1−), apymt = 4-aminopyrimidine-2-thionate(1−), dapymt = 4,6-diaminopyrimidine-2-thionate(1−), or mpol = 2-sulfanyl-3-pyridinolate(2−)] were carried out and the products characterized by UV/vis, NMR spectroscopy, electrospray ionization mass spectrometry, and crystal structure analysis. All products are dinuclear rhodium(III) complexes of $[\{Rh(\eta^5\text{-}C_5Me_5)(L)\}_2]^{n+}$: three crystal structures with mpymt, dmpymt and mpol were determined. The mpymt and dmpymt ligands co-ordinate through a $1\kappa^2N,S:2\kappa S$ mode and the two pyrimidine rings are located in *cis* position, whereas mpol adopts a five-membered chelating mode with $1\kappa^2S,O:2\kappa S$ and the two pyrimidine rings are located in *trans* position. Such structural difference can reasonably be explained by the intramolecular stacking interaction between the two bridging ligands.

Introduction

The synthetic strategies based on self-assembling reactions are very important to synthesize supramolecular compounds.[1] Our recent studies showed that cyclic tri- and tetra-nuclear cobalt(III) complexes $[Co_n(put\text{-}N,S,N')_n(tacn)_n]X_n$ could be prepared from the reaction of *fac*-$[CoCl_3(tacn)]$ (tacn = 1,4,7-triazacyclononane) and 9*H*-purine-6(1*H*)-thione (H_2put) in the presence of an equimolar amount of NaOH.[2] Here we will report similar kinds of self-assembling reactions between $[Rh(\eta^5\text{-}C_5Me_5)(H_2O)_3]^{2+}$ and pyrimidine-2-thionate or related ligands instead of H_2put.

Pyrimidine-2-thionate is a very interesting ligand and adopts many kinds of co-ordination modes. Scheme 1 shows the possible modes for oligomeric structure formation: **A**,[3] **B**,[4] and **C**

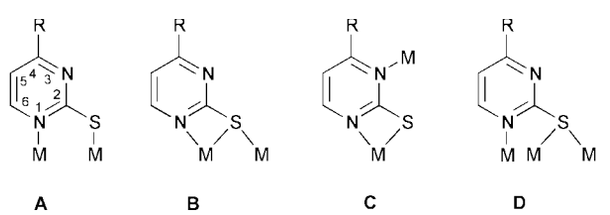

(unknown) bridge between two metals and **D**[5] between three metals. The nuclearity of the product may largely depend on which of the bridging modes will be adopted. Six bridging ligands were used: pyrimidine-2-thione (Hpymt), 4-methyl-pyrimidine-2-thione (Hmpymt), 4,6-dimethylpyrimidine-2-thione (Hdmpymt), 4-aminopyrimidine-2-thione (Hapymt), 4,6-diaminopyrimidine-2-thione (Hdapymt), and 2-sulfanyl-3-pyridinol (H_2mpol).

Results and discussion

Preparation of complexes

The reaction of $[Rh(\eta^5\text{-}C_5Me_5)(H_2O)_3]^{2+}$ and Hpymt in the presence of an equimolar amount of NaOH will produce $[Rh(\eta^5\text{-}C_5Me_5)(pymt\text{-}N,S)(H_2O)]^+$ at first. The pymt ligand still has a co-ordinating ability after co-ordination to Rh^{III}, as does Hput. Hence, the subsequent self-assembling process will be expected to lead to cyclic polynuclear complexes $[\{Rh(\eta^5\text{-}C_5Me_5)(pymt)\}_n]^{n+}$. Scheme 1 illustrates this synthetic

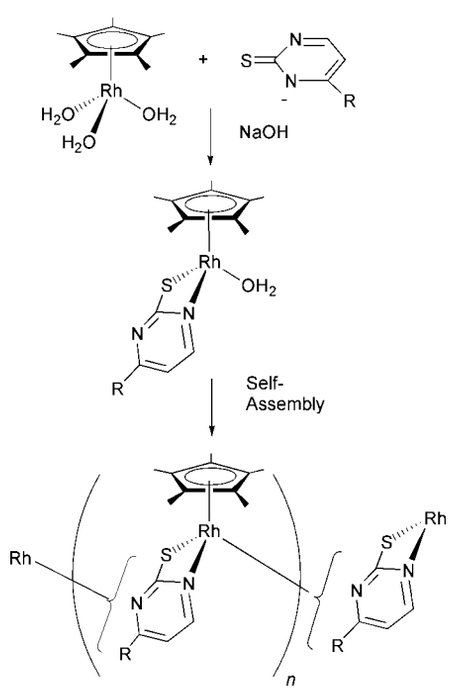

Scheme 1

strategy: the most crucial point is the co-ordination mode adopted by the bridging ligand. When the mode **B** is adopted the product is restricted to a dinuclear structure. When the

Table 1 The ^{1}H NMR, UV/vis and ESI mass spectral data of $[\{Rh(C_5Me_5)(L)\}_2]^{n+}$ **1**–**6**

Complex	NMR (δ)[a]		UV/vis[b]	ESI MS[c]
	C_5Me_5	pymt	λ/nm (ε/dm^3 mol^{-1} cm^{-1})	*m*/*z*
1 $[\{Rh(C_5Me_5)(pymt)\}_2][PF_6]_2$	1.82 (s, 15 H)	7.27 (t, 1 H)	387 (10600)	349 $[M - X]^+$
		8.66 (dd, 1 H)	*ca.* 280 (sh) (30400)	390 $[M - X + AN]^+$
		8.77 (dd, 1 H)	250 (43000)	843 $[2M - X]^+$
2 $[\{Rh(C_5Me_5)(mpymt)\}_2][ClO_4]_2$	1.81 (s, 15 H)	2.42 (s, 3 H)	391 (10500)	363 $[M - X]^+$, $[M - 2X]^{2+}$
		7.18 (d, 1 H)	*ca.* 280 (sh) (32000)	404 $[M - X + AN]^+$
		8.60 (dd, 1 H)	250 (44200)	825 $[2M - X]^+$
				866 $[2M - X + AN]^+$
3 $[\{Rh(C_5Me_5)(dmpymt)\}_2][PF_6]_2$	1.83 (s, 15 H)	2.37 (s, 3 H)	395 (10400)	377 $[M - X]^+$, $[2M - 2X]^{2+}$
		2.39 (s, 3 H)	*ca.* 285 (sh) (30000)	418 $[M - X + AN]^+$
		7.09 (s, 1 H)	254 (44000)	899 $[2M - X]^+$
4 $[\{Rh(C_5Me_5)(apymt)\}_2][PF_6]_2$	1.79 (s, 15 H)	6.16 (d, 1 H)	397 (11200)	364 $[2M - 2X]^{2+}$
		7.58 (s, 2 H)	*ca.* 324 (sh) (17400)	405 $[M - X + AN]^+$
		7.87 (d, 1 H)	*ca.* 285 (sh) (38800)	873 $[2M - X]^+$
			250 (65500)	
5 $[\{Rh(C_5Me_5)(dapymt)\}_2][PF_6]_2$	1.82 (s, 15 H)	5.27 (s, 1 H)	397 (10000)	379 $[2M - 2X]^{2+}$
		5.95 (s, 2 H)	*ca.* 285 (sh) (23300)	857 $[2M - X]^+$
		6.76 (s, 2 H)	248 (60600)	
6 $[\{Rh(C_5Me_5)(mpol)\}_2]$	1.16 (s, 15 H)	6.74 (q, 1 H)	390 (18600)	364 $[M + H]^+$
		6.87 (dd, 1 H)	305 (sh) (20900)	727 $[2M + H]^+$
		7.40 (dd, 1 H)	266 (37100)	749 $[2M + Na]^+$
			233 (38700)	1090 $[3M + H]^+$

[a] Downfield relative to $SiMe_4$ in $(CD_3)_2SO$. [b] Measured in water. [c] Positive ESI measured in acetonitrile; M = $[Rh(C_5Me_5)(L)][X]$ and AN = acetonitrile.

mode **C** is adopted it is possible to form nuclearities higher than $n = 3$.

In the case of each ligand only one complex was obtained in a good yield. Proton NMR data of the complexes **1**–**6** are shown in Table 1. Each complex showed a single methyl signal due to η^5-C_5Me_5 and one set of signals due to the bridging ligand. Therefore, each complex is composed of a single species. It should be noted that the methyl signal of η^5-C_5Me_5 in complexes **1**–**5** with pyrimidine-2-thionato ligand appeared at δ 1.79–1.83, whereas complex **6** exhibited it at δ 1.16. Such a large chemical shift difference suggests a significant structural difference. The elemental analyses of all complexes are consistent with the composition $[\{Rh(\eta^5\text{-}C_5Me_5)(L)\}_n]X_n$. The determination of *n*, however, is impossible by elemental analysis and ESI mass spectral measurements were attempted.

The UV/vis absorption spectral data are shown in Table 1. All the pymt complexes show similar spectra. There are mainly three components at 387–397, *ca*. 280–285 and 250 nm. Since these bands have large molar absorption coefficients they are assignable to transitions with charge-transfer characters.

ESI Mass spectra

Fig. 1 shows a positive ESI mass spectrum of complex **4** in acetonitrile. The *m*/*z* values given in the text refer to calculated masses. The dominant peaks at *m*/*z* = 364 and 873 correspond to the ions $[2M - 2X]^{2+}$ and $[2M - X]^+$, respectively, where M indicates $[Rh(\eta^5\text{-}C_5Me_5)(apymt)]PF_6$ and X a counter ion. The peak at *m*/*z* = 405 corresponds to the ion $[M - X + AN]^+$ (AN = acetonitrile). These results indicate that the complex **4** has a dinuclear composition ($n = 2$).

The other complexes **1**–**3** and **5** showed similar ESI mass spectra (Table 1). The largest *m*/*z* peak $[2M - X]^+$, which corresponds to the dinuclear composition, was observed for all complexes. Hence we can conclude that all pyrimidine-2-thionato complexes **1**–**5** are dinuclear. Some mononuclear peaks such as $[M - X]^+$ and/or $[M - X + AN]^+$ were also observed. They were, however, generated from the decomposition of the dinuclear complexes because all complexes are composed of single species as shown by ^{1}H NMR measurements.

Complex **6** is a neutral molecule but its positive ESI mass spectrum showed some peaks. The peaks at *m*/*z* = 364, 727, 749 and 1090 correspond to the ions $[M + H]^+$, $[2M + H]^+$, $[2M + Na]^+$ and $[3M + H]^+$, respectively. Although the peak intensity corresponding to the dinuclear composition $[2M + H]^+$ was the strongest, we could not eliminate the possibility of the trinuclear composition from the ESI mass spectrum. It was finally determined by crystal analysis described below.

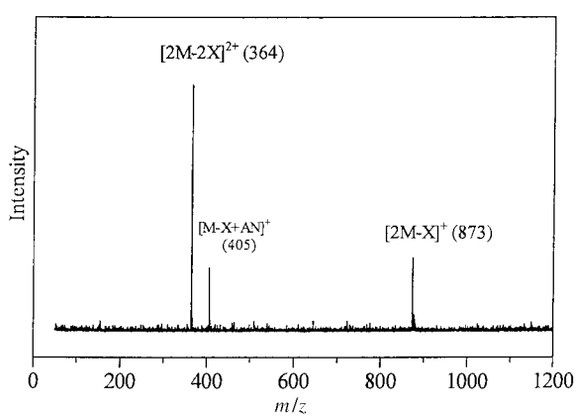

Fig. 1 Positive ESI mass spectrum of complex **4** measured in acetonitrile; M = $[Rh(\eta^5\text{-}C_5Me_5)(apymt)][PF_6]$.

Crystal structures of $[\{Rh(\eta^5\text{-}C_5Me_5)(mpymt)\}_2][ClO_4]_2$ **2** and $[\{Rh(\eta^5\text{-}C_5Me_5)(dmpymt)\}_2][PF_6]_2\cdot(CH_3)_2CO$ **3**

As described in the Experimental section, significant disorders were observed in the structures of complexes **2** and **3**. This is clearly shown in Fig. 2 of the structure of **2**: there are two sites for each of the bridging mpymt ligands. The occupancy of site "a" was fixed to 65% and that of "b" to 35%. Figs. 3 and 4 show the numbered ORTEP[6] drawings of complex ions at site "a" in **2** and **3**, respectively. The two crystal structures are isomorphous though complex **3** contains one solvent acetone. Selected bond distances and angles are listed in Table 2.

Both structures consist of a dimer of two rhodium atoms bridged by the two sulfur atoms. The pentamethylcyclopentadienyl residues adopt the usual η^5 co-ordination mode. The ligands, mpymt and dmpymt, co-ordinate to one Rh^{III} in a bidentate manner through the 1-nitrogen and 2-sulfur donors

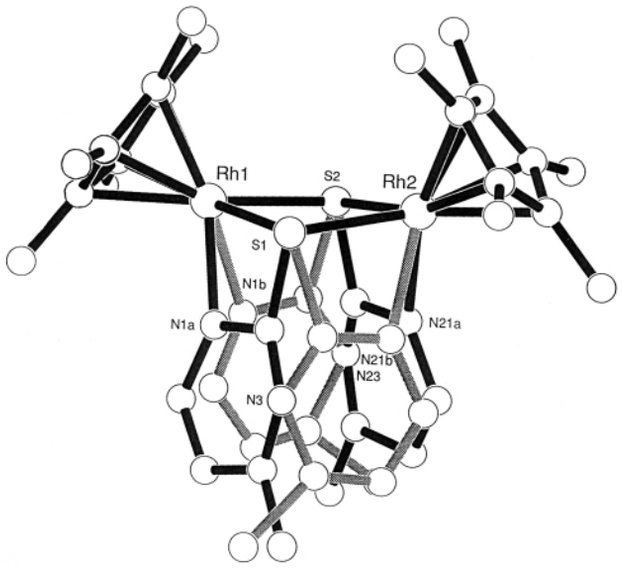

Fig. 2 Disorders of $[\{Rh(\eta^5\text{-}C_5Me_5)(mpymt)\}_2][ClO_4]_2$ **2**: the occupancies of sites "a" and "b" are 65 and 35%, respectively. The bridging S(1) and S(2) atoms and the two N(3) and N(23) atoms are accidentally degenerate.

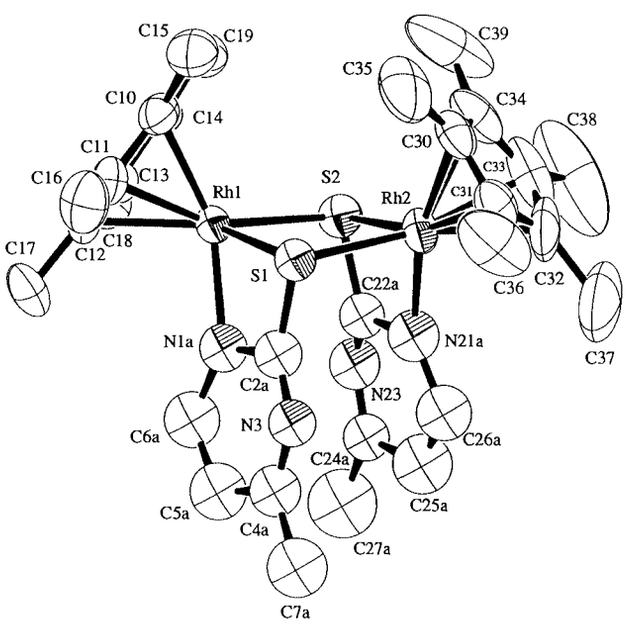

Fig. 3 An ORTEP drawing of the cation at site "a" in complex **2**.

and bridge the other Rh^{III} through the 2-sulfur donor. The 3-nitrogen donor atom does not take part in co-ordination. Complexes **2** and **3** adopt mode **B** ($1\kappa^2N,S:2\kappa S$ and $1\kappa S:2\kappa^2N,S$), which leads to the dinuclear structure. The two η^5-C_5Me_5 rings are located in *cis* position and the bridging ligands are just face-to-face on the same side.

In complex **2** (Fig. 3) the central Rh_2S_2 core forms a square [Rh · · · Rh 3.584(1), S(1) · · · S(2) 3.302(3) Å, Rh(1)–S(1)–Rh(2) 94.53(8), Rh(1)–S(2)–Rh(2) 94.20(8), S(1)–Rh(1)–S(2) 84.85(8) and S(1)–Rh(2)–S(2) 85.22(8)°]. The Rh and S atoms deviate slightly, above and below, respectively, from the mean Rh_2S_2 plane. The bridging two Rh–S distances are almost equal: Rh(1)–S(1) 2.449(2), Rh(1)–S(2) 2.446(2), Rh(2)–S(1) 2.430(2), and Rh(2)–S(2) 2.447(3) Å. These distances are slightly longer than 2.394(4) Å in $[Rh(\eta^5\text{-}C_5Me_5)(\eta^2\text{-}2\text{-}SC_5H_3N\text{-}3\text{-}SiMe_3)_2]$[7] and average 2.379 Å in *mer*-$[Rh(pyt)_3]$ (Hpyt = pyridine-2-thiol).[8] The Rh–N lengths [2.09(1) and 2.11(1) Å] are normal but the e.s.d.s are large owing to the disordered structure. The average Rh–C distances [2.158 for Rh(1) and 2.144 Å for Rh(2)] are unexceptional: the thermal vibrations in

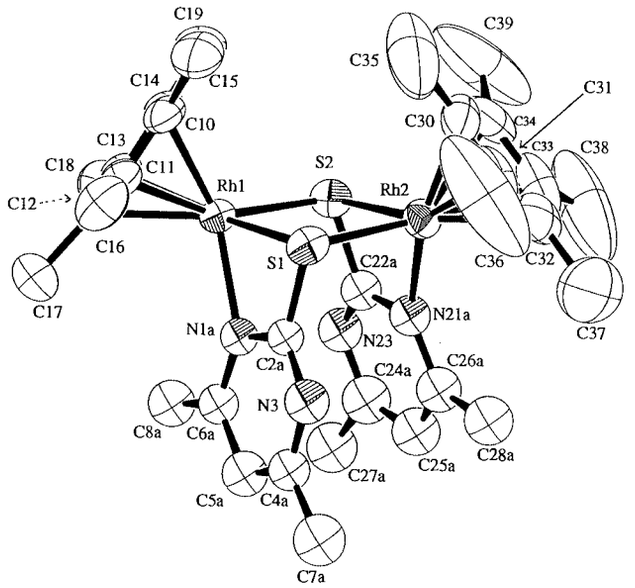

Fig. 4 An ORTEP drawing of the cation at site "a" in $[\{Rh(\eta^5\text{-}C_5Me_5)(dmpymt)\}_2][PF_6]_2\cdot(CH_3)_2CO$ **3**.

the η^5-C_5Me_5 ring of C(30)–C(39) are larger than those of C(10)–C(19) as shown by their thermal ellipsoids. The major structural distortions are the S–Rh–N bite angles of 66.7(4) and 65.9(4)°, which are the consequence of the four-membered chelate ring formation.

The *cis* structure apparently seems to be unfavourable due to the steric congestion of the two bridging ligands and the other *trans* structure where each of the bridging ligands is located above and below the Rh_2S_2 plane seems to be favourable. However, there is an intramolecular stacking interaction between these two bridging ligands in the *cis* structure. Fig. 5 demonstrates the effective overlap of two pyrimidine rings, which will be a driving force stabilizing the *cis* structure. The distances N(1a) · · · C(22a), N(21a) · · · C(2a), N(23) · · · C(6a) and N(3) · · · C(26a) are 2.96(2), 2.91(2), 3.53(2) and 3.31(2) Å, respectively, in complex **2**, and 3.02(2), 3.05(2), 3.49(2) and 3.65(2) Å, respectively, in **3**.

The other complexes, **1**, **4**, and **5** have been assigned the dinuclear structure from the ESI mass spectra. It is reasonable that these adopt the same *cis* structure as that of **2** and **3** because all the complexes are expected to have two four-membered chelate rings and hence the effective intramolecular stacking interaction between the two pyrimidine rings as shown in Fig. 5. Another support is given by ^1H NMR spectra: complexes **1**–**5** showed the methyl signal of η^5-C_5Me_5 at the same magnetic field region of δ 1.79–1.83, largely different from δ 1.16 of **6** with *trans* structure as described below.

Crystal structure of $[\{Rh(\eta^5\text{-}C_5Me_5)(mpol)\}_2]\cdot 3H_2O$ 6

Complex **6** contains two crystallographically independent molecules and each has a center of symmetry. The thermal ellipsoids of η^5-C_5Me_5 in the Rh(2) structure are a little larger than those in the Rh(1) structure but the fundamental structures are quite similar. Fig. 6 shows the numbered ORTEP[6] drawing of the Rh(1) structure in $[\{Rh(\eta^5\text{-}C_5Me_5)(mpol)\}_2]\cdot 3H_2O$ **6**. Selected bond distances and angles are listed in Table 2.

The structure consists of a dimer of two rhodium atoms bridged by the two sulfur atoms. Since there is an inversion center between the two rhodium(III) ions these two sites are completely equivalent. The mpol ligand co-ordinates to one Rh^{III} in a bidentate manner through the 2-sulfur and 3-oxygen donors and bridges the other Rh^{III} through the 2-sulfur donor. In complex **6** the 1-nitrogen donor does not participate in co-

Table 2 Selected bond distances (Å) and bond angles (°) of [{Rh(η^5-C_5Me_5)(mpymt)}$_2$][ClO_4]$_2$ **2**, [{Rh(η^5-C_5Me_5)(dmpymt)}$_2$][PF_6]$_2$·$(CH_3)_2CO$ **3** and [{Rh(η^5-C_5Me_5)(mpol)}$_2$]·3H_2O **6**

2		**3**		**6**	
Rh(1)–C(10)	2.149(9)	Rh(1)–C(10)	2.137(8)	Rh(1)–C(6)	2.156(3)
Rh(1)–C(11)	2.153(9)	Rh(1)–C(11)	2.154(8)	Rh(1)–C(7)	2.164(3)
Rh(1)–C(12)	2.171(8)	Rh(1)–C(12)	2.183(8)	Rh(1)–C(8)	2.153(3)
Rh(1)–C(13)	2.144(9)	Rh(1)–C(13)	2.163(8)	Rh(1)–C(9)	2.190(3)
Rh(1)–C(14)	2.172(9)	Rh(1)–C(14)	2.163(8)	Rh(1)–C(10)	2.185(3)
Rh(2)–C(30)	2.152(9)	Rh(2)–C(30)	2.11(1)	Rh(2)–C(26)	2.130(4)
Rh(2)–C(31)	2.14(1)	Rh(2)–C(31)	2.15(1)	Rh(2)–C(27)	2.163(4)
Rh(2)–C(32)	2.15(1)	Rh(2)–C(32)	2.16(1)	Rh(2)–C(28)	2.149(3)
Rh(2)–C(33)	2.14(1)	Rh(2)–C(33)	2.16(1)	Rh(2)–C(29)	2.192(3)
Rh(2)–C(34)	2.14(1)	Rh(2)–C(34)	2.12(1)	Rh(2)–C(30)	2.160(4)
Rh(1)–S(1)	2.449(2)	Rh(1)–S(1)	2.445(2)	Rh(1)–S(1)	2.365(1)
Rh(1)–S(2)	2.446(2)	Rh(1)–S(2)	2.430(2)	Rh(1)–S(1)*	2.3986(7)
Rh(2)–S(1)	2.430(2)	Rh(2)–S(1)	2.441(2)	Rh(2)–S(2)	2.370(1)
Rh(2)–S(2)	2.447(3)	Rh(2)–S(2)	2.441(2)	Rh(2)–S(2)*	2.4064(8)
Rh(1)–N(1a)	2.09(1)	Rh(1)–N(1a)	2.13(1)	Rh(1)–O(1)	2.093(2)
Rh(2)–N(21a)	2.11(1)	Rh(2)–N(21a)	2.13(1)	Rh(2)–O(2)	2.105(2)
S(1)–C(2a)	1.68(2)	S(1)–C(2a)	1.72(1)	S(1)–C(1)	1.779(3)
N(1a)–C(2a)	1.46(2)	N(1a)–C(2a)	1.33(1)	N(1)–C(1)	1.329(4)
C(2a)–N(3)	1.26(2)	C(2a)–N(3)	1.34(1)	C(1)–C(2)	1.407(5)
N(3)–C(4a)	1.28(2)	N(3)–C(4a)	1.34(2)	C(2)–O(1)	1.322(4)
C(4a)–C(7a)	1.45(3)	C(4a)–C(7a)	1.52(2)	C(2)–C(3)	1.408(4)
C(4a)–C(5a)	1.45(3)	C(4a)–C(5a)	1.37(2)	C(3)–C(4)	1.381(6)
C(5a)–C(6a)	1.42(3)	C(5a)–C(6a)	1.44(2)	C(4)–C(5)	1.376(7)
		C(6a)–C(8a)	1.47(2)		
C(6a)–N(1a)	1.46(2)	C(6a)–N(1a)	1.36(2)	C(5)–N(1)	1.338(5)
S(2)–C(22a)	1.72(2)	S(2)–C(22a)	1.72(1)	S(2)–C(21)	1.769(3)
N(21a)–C(22a)	1.43(2)	N(21a)–C(22a)	1.33(2)	N(2)–C(21)	1.334(4)
C(22a)–N(23)	1.22(2)	C(22a)–N(23)	1.31(1)	C(21)–C(22)	1.426(5)
N(23)–C(24a)	1.24(2)	N(23)–C(24a)	1.30(2)	C(22)–O(2)	1.315(4)
C(24a)–C(27a)	1.56(3)	C(24a)–C(27a)	1.59(3)	C(22)–C(23)	1.396(5)
C(24a)–C(25a)	1.53(3)	C(24a)–C(25a)	1.39(2)	C(23)–C(24)	1.382(6)
C(25a)–C(26a)	1.43(3)	C(25a)–C(26a)	1.40(2)	C(24)–C(25)	1.361(7)
		C(26a)–C(28a)	1.49(2)		
C(26a)–N(21a)	1.39(2)	C(26a)–N(21a)	1.37(2)	C(25)–N(2)	1.354(5)
S(1)–Rh(1)–N(1a)	66.7(4)	S(1)–Rh(1)–N(1a)	67.0(3)	S(1)–Rh(1)–O(1)	82.37(7)
S(2)–Rh(2)–N(21a)	65.9(4)	S(2)–Rh(2)–N(21a)	65.9(3)	S(2)–Rh(2)–O(2)	82.32(6)
Rh(1)–S(1)–Rh(2)	94.53(8)	Rh(1)–S(1)–Rh(2)	94.59(8)	Rh(1)–S(1)–Rh(1)*	96.13(3)
Rh(1)–S(2)–Rh(2)	94.20(8)	Rh(1)–S(2)–Rh(2)	94.98(8)	Rh(2)–S(2)–Rh(2)*	94.98(4)
S(1)–Rh(1)–S(2)	84.85(8)	S(1)–Rh(1)–S(2)	85.16(8)	S(1)–Rh(1)–S(1)*	83.87(3)
S(1)–Rh(2)–S(2)	85.22(8)	S(1)–Rh(2)–S(2)	85.00(7)	S(2)–Rh(2)–S(2)*	85.02(4)
Rh(1)–S(1)–C(2a)	83.7(6)	Rh(1)–S(1)–C(2a)	79.6(4)	Rh(1)–S(1)–C(1)	94.9(1)
S(1)–C(2a)–N(1a)	106(1)	S(1)–C(2a)–N(1a)	112.2(9)	S(1)–C(1)–C(2)	116.8(2)
Rh(1)–N(1a)–C(2a)	103(1)	Rh(1)–N(1a)–C(2a)	101.0(7)	C(1)–C(2)–O(1)	121.8(3)
C(2a)–N(1a)–C(6a)	121(1)	C(2a)–N(1a)–C(6a)	121(1)	Rh(1)–O(1)–C(2)	114.7(2)
N(1a)–C(2a)–N(3)	118(1)	N(1a)–C(2a)–N(3)	124(1)	N(1)–C(1)–C(2)	125.1(3)
C(2a)–N(3)–C(4a)	128(1)	C(2a)–N(3)–C(4a)	119(1)	C(1)–C(2)–C(3)	116.1(3)
N(3)–C(4a)–C(5a)	117(2)	N(3)–C(4a)–C(5a)	120(1)	C(2)–C(3)–C(4)	118.6(4)
C(4a)–C(5a)–C(6a)	122(2)	C(4a)–C(5a)–C(6a)	120(1)	C(3)–C(4)–C(5)	120.4(3)
C(5a)–C(6a)–N(1a)	113(2)	C(5a)–C(6a)–N(1a)	116(1)	N(1)–C(5)–C(4)	122.6(4)
Rh(2)–S(2)–C(22a)	84.3(6)	Rh(2)–S(2)–C(22a)	81.1(4)	C(1)–N(1)–C(5)	117.3(3)
S(2)–C(22a)–N(21a)	104(1)	S(2)–C(22a)–N(21a)	110(1)	Rh(2)–S(2)–C(21)	94.3(1)
Rh(2)–N(21a)–C(22a)	105(1)	Rh(2)–N(21a)–C(22a)	103.4(8)	S(2)–C(21)–C(22)	117.7(2)
C(22a)–N(21a)–C(26a)	122(2)	C(22a)–N(21a)–C(26a)	120(1)	C(21)–C(22)–O(2)	120.7(3)
N(21a)–C(22a)–N(23)	118(2)	N(21a)–C(22a)–N(23)	125(1)	Rh(2)–O(2)–C(22)	114.6(2)
C(22a)–N(23)–C(24a)	131(1)	C(22a)–N(23)–C(24a)	120(1)	N(2)–C(21)–C(22)	123.9(3)
N(23)–C(24a)–C(25a)	111(2)	N(23)–C(24a)–C(25a)	120(2)	C(21)–C(22)–C(23)	116.1(3)
C(24a)–C(25a)–C(26a)	123(2)	C(24a)–C(25a)–C(26a)	121(2)	C(22)–C(23)–C(24)	119.6(4)
C(25a)–C(26a)–N(21a)	111(1)	C(25a)–C(26a)–N(21a)	115(1)	C(23)–C(24)–C(25)	120.1(4)
				N(2)–C(25)–C(24)	122.8(3)
				C(21)–N(2)–C(25)	117.4(3)

ordination. The present S,O chelating mode seems to be popular in other mpol complexes.[9] The two η^5-C_5Me_5 rings are located in *trans* position and the bridging ligands also become *trans*. This *trans* structure is in contrast to the *cis* one of complexes **2** and **3**. Complex **6** has two five-membered chelate rings and if it were to adopt the *cis* structure there would be no effective intramolecular stacking interaction between the two bridging heterocyclic rings. Thus it adopts the *trans* structure because of small steric congestion. It is noteworthy that there is an intramolecular CH–π interaction[10] between the mpol ring and one of the methyl groups of η^5-C_5Me_5: the distances N(1)···C(13), C(1)···C(13) and C(2)···C(13) are 3.655(6), 3.441(5) and 3.483(5) Å, respectively. This interaction partly contributes to the stabilization of the *trans* structure. The higher magnetic field shift (*ca.* 0.65 ppm) of the C_5Me_5 methyl signal of the *trans* structure is due to this intramolecular CH–π interaction.

In complex **6** the central Rh_2S_2 core forms a square [Rh(1)···Rh(1)* 3.544(2) Å, Rh(1)–S(1)–Rh(1)* 96.13(3) and S(1)–Rh(1)–S(1)* 83.87(3)°] and is completely in the same plane. The bridging Rh–S distances are 2.365(1) and 2.3986(7) Å, which are shorter than those of complexes **2** and **3** and

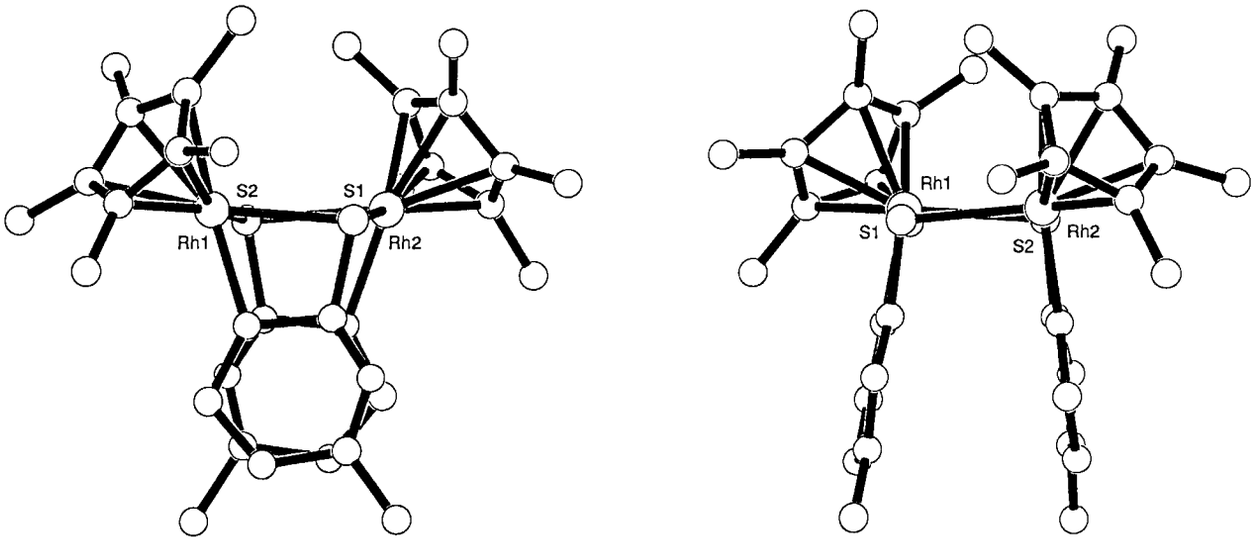

Fig. 5 Two side views of the intramolecular π–π stacking interaction in $[\{Rh(\eta^5\text{-}C_5Me_5)(mpymt)\}_2][ClO_4]_2$ **2**.

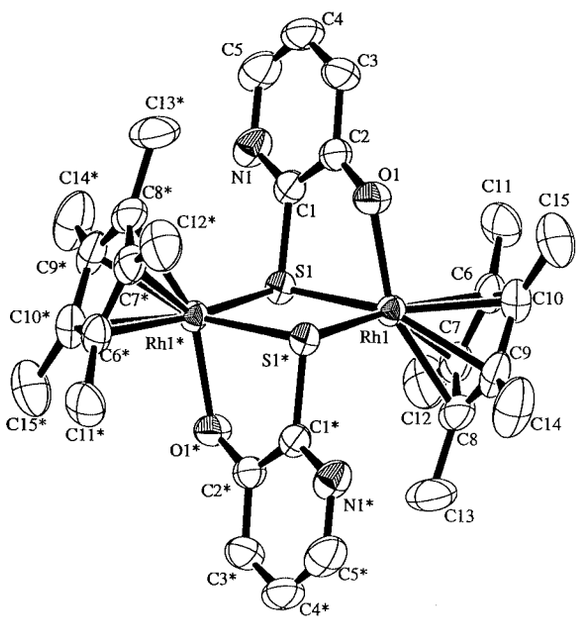

Fig. 6 An ORTEP drawing of $[\{Rh(\eta^5\text{-}C_5Me_5)(mpol)\}_2]\cdot 3H_2O$ **6**.

similar to average 2.379 Å in *mer*-$[Rh(pyt)_3]$.[8] The Rh–O length [2.093(2) Å] and the average Rh–C distances [2.170 Å] are normal values. The bite angle S(1)–Rh(1)–O(1) is 82.37(7)°, which is considerably larger than *ca.* 66–67° of complexes **2** and **3** with four-membered chelate rings.

Conclusion

The present reactions of $[Rh(\eta^5\text{-}C_5Me_5)(H_2O)_3]^{2+}$ and Hpymt produced only dinuclear complexes $[\{Rh(\eta^5\text{-}C_5Me_5)(pymt)\}_n]^{n+}$. All the pymt complexes adopt the $1\kappa^2N,S:2\kappa S$ and $1\kappa S:2\kappa^2N,S$ co-ordination, that is mode **B**. The preference of the N(1)/S^2 mode rather than the S^2/N(3) one has generally been seen in other complexes containing cobalt(III)[11] and ruthenium(II)[12] ions. The bridging ability of the N(3) atom seems to be relatively weak in the present rhodium(III)–pyrimidine-2-thione system. 2-Thiouracil (H_2tuc = 2,3-dihydro-2-thioxo-1*H*-pyrimidin-4-one) has a similar ligand skeleton to pyrimidine-2-thione but its chemistry is considerably different.[11,12] For example, the tuc complexes adopt the S^2/N(3) co-ordination mode rather than the N(1)/S^2 one. Comparison of these two ligand systems will be intriguing and is now in progress.

Experimental

Preparation of complexes

All of the thione ligands (Aldrich) were used without further purification. The starting material $[\{Rh(\eta^5\text{-}C_5Me_5)Cl_2\}_2]$ was prepared according to the literature.[13]

$[\{Rh(\eta^5\text{-}C_5Me_5)(pymt)\}_2][PF_6]_2$ 1, $[\{Rh(\eta^5\text{-}C_5Me_5)(dmpymt)\}_2][PF_6]_2$ 3 and $[\{Rh(\eta^5\text{-}C_5Me_5)(apymt)\}_2][PF_6]_2\cdot H_2O$ 4. The general preparation method was as follows. To a suspension of $[\{Rh(\eta^5\text{-}C_5Me_5)Cl_2\}_2]$ (0.2 g, 0.32 mmol) in water (30 cm^3) was added silver hexafluorophosphate (0.26 g, 1.3 mmol) and the mixture stirred at 40 °C for 1 h. The resulting precipitate of silver chloride was removed by filtration and to the filtrate was added a 50% aqueous/ethanol solution (50 cm^3) of Hpymt (0.072 g, 0.64 mmol) adjusted to pH 8–9 by adding aqueous NaOH. The mixed solution was refluxed at 80 °C for 3 h then cooled to room temperature and addition of NH_4PF_6 (0.3 g) gave the red-orange hexafluorophosphate salt which was recrystallized from water and ethanol. The yields were 60–80%. Found: C, 34.40; H, 3.75; N, 5.88. Calc. for $[\{Rh(\eta^5\text{-}C_5Me_5)(pymt)\}_2][PF_6]_2$ **1** ($C_{14}H_{18}F_6N_2PRhS$): C, 34.02; H, 3.67, N, 5.67%. Found: C, 36.91; H, 4.34; N, 5.39. Calc. for $[\{Rh(\eta^5\text{-}C_5Me_5)(dmpymt)\}_2][PF_6]_2$ **3** ($C_{16}H_{22}F_6N_2PRhS$): C, 36.79; H, 4.25, N, 5.36%. Found: C, 32.52; H, 3.86; N, 8.18. Calc. for $[\{Rh(\eta^5\text{-}C_5Me_5)(apymt)\}_2][PF_6]_2\cdot H_2O$ **4** ($C_{28}H_{40}F_{12}N_6OP_2Rh_2S_2$): C, 32.45; H, 3.89, N, 8.11%.

$[\{Rh(\eta^5\text{-}C_5Me_5)(mpymt)\}_2][ClO_4]_2\cdot H_2O$ 2 and $[\{Rh(\eta^5\text{-}C_5Me_5)(dapymt)\}_2][ClO_4]_2\cdot H_2O$ 5. In these preparations silver perchlorate was used instead of silver hexafluorophosphate and hence these two complexes were isolated as the perchlorate salts. Found: C, 38.55; H, 4.51; N, 5.99. Calc. for $[\{Rh(\eta^5\text{-}C_5Me_5)(mpymt)\}_2][ClO_4]_2\cdot H_2O$ **2** ($C_{30}H_{42}Cl_2N_4O_9Rh_2S_2$): C, 38.19; H, 4.49; N, 5.94%. Found: C, 34.22; H, 4.26; N, 11.58. Calc. for $[\{Rh(\eta^5\text{-}C_5Me_5)(dapymt)\}_2][ClO_4]_2\cdot H_2O$ **5** ($C_{28}H_{42}Cl_2N_8O_9Rh_2S_2$): C, 34.47; H, 4.34; N, 11.49%.

$[\{Rh(\eta^5\text{-}C_5Me_5)(mpol)\}_2]\cdot 3H_2O$ 6. To a suspended solution of $[\{Rh(\eta^5\text{-}C_5Me_5)Cl_2\}_2]$ (0.2 g, 0.32 mmol) in water (30 cm^3) was added silver hexafluorophosphate (0.26 g, 1.3 mmol) and the mixture stirred at 40 °C for 1 h. The resulting precipitate of silver chloride was removed by filtration and to the filtrate was added a 50% aqueous/ethanol solution (60 cm^3) of H_2mpol (0.081 g, 0.64 mmol) adjusted to pH 8–9 by adding aqueous NaOH. The mixed solution was refluxed at 80 °C for 4 h, then cooled to room temperature, concentrated to small volume by a

Table 3 Crystallographic data for $[\{Rh(\eta^5\text{-}C_5Me_5)(mpymt)\}_2][ClO_4]_2$ **2**, $[\{Rh(\eta^5\text{-}C_5Me_5)(dmpymt)\}_2][PF_6]_2\cdot(CH_3)_2CO$ **3** and $[\{Rh(\eta^5\text{-}C_5Me_5)(mpol)\}_2]\cdot 3H_2O$ **6**

	2	**3**	**6**
Formula	$C_{30}H_{40}Cl_2N_4O_8Rh_2S_2$	$C_{35}H_{50}F_{12}N_4OP_2Rh_2S_2$	$C_{30}H_{42}N_2O_5Rh_2S_2$
Formula weight	925.51	1102.67	780.60
T/K	295	295	295
Space group	$P2_1/a$ (no. 14)	$P2_1/a$ (no. 14)	$P\bar{1}$ (no. 2)
Crystal system	Monoclinic	Monoclinic	Triclinic
a/Å	15.164(3)	15.727(4)	11.101(6)
b/Å	12.762(4)	13.366(3)	16.935(7)
c/Å	21.467(3)	21.707(2)	9.974(4)
α/°			95.32(4)
β/°	108.04(1)	98.32(1)	110.15(4)
γ/°			107.24(3)
V/Å^3	3950(1)	4514(1)	1641(1)
Z	4	4	2
μ(Mo-Kα)/cm^{-1}	11.23	9.75	11.70
Reflections collected	11930	8274	9882
Reflections observed [$I > 3\sigma I$]	4700	5128	8036
R	0.053	0.052	0.033
R_w	0.070	0.069	0.051

rotatory evaporator and kept standing overnight to give a red precipitate. The crude product was recrystallized from ethanol. The yield was *ca*. 80%. Found: C, 45.66; H, 5.35; N, 3.61. Calc. for $[\{Rh(\eta^5\text{-}C_5Me_5)(mpol)\}_2]$ **6** ($C_{30}H_{42}N_2O_5Rh_2S_2$): C, 46.16; H, 5.42; N, 3.59%.

CAUTION: In general, perchlorate salts of metal complexes with organic ligands are potentially explosive and should be handled with great care.

ESI Mass spectral measurements

ESI mass spectra were obtained by a sector-type mass spectrometer (JEOL-D300) connected with a laboratory-made ESI interface.[14] A sample solution is sprayed from the tip of a needle by applying a voltage 3.5 kV higher than that of a counter electrode. The distance between the needle and the counter electrode was 1 cm. The counter electrode consists of a 12 cm long stainless steel capillary tube (0.5 mm i.d.). A stream of heated N_2 gas (70 °C) was used to aid desolvation of sprayed charged droplets. The flow rate of the sample solution was 2 μl min^{-1} and the cone voltage 50 eV. For measurements of ESI mass spectra, the perchlorate and hexafluorophosphate salts were used because of their higher solubilities in organic solvents. The samples were dissolved in freshly distilled acetonitrile or methanol and nothing was added to promote ionization. The concentrations of samples were kept at *ca.* 10^{-4} mol dm^{-3}.

Crystal structure determinations of $[\{Rh(\eta^5\text{-}C_5Me_5)(mpymt)\}_2][ClO_4]_2$ 2, $[\{Rh(\eta^5\text{-}C_5Me_5)(dmpymt)\}_2][PF_6]_2\cdot(CH_3)_2CO$ 3 and $[\{Rh(\eta^5\text{-}C_5Me_5)(mpol)\}_2]\cdot 3H_2O$ 6

A red plate crystal of complex **2**, and a red column crystal of **3**, were grown from $(CH_3)_2CO$–Et_2O at room temperature. A red prismatic crystal of **6** was grown from MeOH–Et_2O at room temperature.

Diffraction data were collected on Rigaku AFC5R (**2**) and AFC7R (**3** and **6**) diffractometers with graphite monochromated Mo-Kα radiation ($\lambda = 0.71069$ Å). Crystallographic data for complexes **2**, **3** and **6** are listed in Table 3. Significant disorders were observed in the structures of **2** and **3**. As shown in Fig. 2 for **2**, there are two sites for the bridging mpymt ligand: the occupancies of sites "a" and "b" are 65 and 35%, respectively. The bridging S(1) and S(2) atoms and the two N(3) and N(23) atoms are accidentally degenerate and hence show 100% site occupancy. Complex **3** showed the same situation as that of **2**. It should be noted that Figs. 3 (complex **2**) and 4 (**3**) show only the structures at site "a". The carbon and nitrogen atoms of the bridging pyrimidine moieties in complexes **2** and **3** were refined isotropically, while the rest were refined anisotropically. One of the perchlorate ions in **2** showed disorder. The phosphorus atom of PF_6^- in complex **3** occupies the same position as the chloride atom of ClO_4^- in **2**. The location of the acetone molecule in complex **3** could not be determined accurately. All calculations were performed using the TEXSAN[15] crystallographic software package.

CCDC reference number 186/1968.

See http://www.rsc.org/suppdata/dt/b0/b000098l/ for crystallographic files in .cif format.

Measurements

The UV/vis absorption spectra were measured in water with a Hitachi 330 spectrophotometer and proton and ^{13}C NMR spectra with JEOL JNM-GSX-270 and GSX-400 spectrometers in $(CD_3)_2SO$. X-Ray crystal analysis was made at the X-Ray Diffraction Service of the Department of Chemistry.

References

1 J.-M. Lehn, *Supramolecular Chemistry*, VCH, Weinheim, 1995.
2 K. Yamanari, I. Fukuda, T. Kawamoto, Y. Kushi, A. Fuyuhiro, N. Kubota, T. Fukuo and R. Arakawa, *Inorg. Chem.*, 1998, **37**, 5611.
3 D. M. L. Goodgame, R. W. Rollins and A. C. Skapski, *Inorg. Chim. Acta*, 1984, **83**, L11.
4 R. Castro, J. A. Garcia-Vazquez, J. Romero, A. Sousa, R. Pritchard and C. A. McAuliffe, *J. Chem. Soc.*, *Dalton Trans.*, 1994, 1115.
5 R. Castro, M. L. Duran, J. A. Garcia-Vazquez, J. Romero, A. Sousa, E. E. Castellano and J. Zukerman-Schpector, *J. Chem. Soc.*, *Dalton Trans.*, 1992, 2559.
6 C. K. Johnson, ORTEP II, Report ORNL-5138, Oak Ridge National Laboratory, Oak Ridge, TN, 1976.
7 E. Block, G. Ofori-Okai, H. Kang, Q. Chen and J. Zubieta, *Inorg. Chim. Acta*, 1991, **190**, 97.
8 P. B. Kettler, Y. Chang, D. Rose, J. Zubieta and M. J. Abrams, *Inorg. Chim. Acta*, 1996, **244**, 199.
9 T.-B. Wen, J.-C. Shi, X. Huang, Z.-N. Chen, Q.-T. Liu and B.-S. Kang, *Polyhedron*, 1998, **17**, 331.
10 M. Nishio, M. Hirota and Y. Umezawa, *The CH–π interaction*, Wiley-VCH, New York, 1998.
11 K. Yamanari, K. Okusako and S. Kaizaki, *J. Chem. Soc.*, *Dalton Trans.*, 1992, 1615; K. Yamanari, K. Okusako, Y. Kushi and S. Kaizaki, *J. Chem. Soc.*, *Dalton Trans.*, 1992, 1621.
12 K. Yamanari, T. Nozaki, A. Fuyuhiro, Y. Kushi and S. Kaizaki, *J. Chem. Soc.*, *Dalton Trans.*, 1996, 2851.
13 C. White, A. Yates and P. M. Maitlis, *Inorg. Synth.*, 1992, **29**, 228.
14 R. Arakawa, S. Tachiyashiki and T. Matsuo, *Anal. Chem.*, 1995, **67**, 4133.
15 TEXSAN-TEXRAY, Structure Analysis Package, Molecular Structure Corporation, Houston, TX, 1985 and 1992.